Anodic Electrosynthesis of a Thin Film of Cu_2S on a Gold Electrode. A Voltammetric, Nanoelectrogravimetric, and *I*/*t* Transient Study

Rodrigo del Río, Daniela Basaure, Ricardo Schrebler, Humberto Gómez, and Ricardo Córdova*

Instituto de Química, Universidad Católica de Valparaíso, Casilla 4059, Valparaíso, Chile

Received: July 9, 2002; In Final Form: October 2, 2002

The electroformation of a Cu_2S phase, obtained by sulfidization of a thin film of copper placed by the spin-coating technique onto the gold surface of a gold/quartz crystal that is part of an electrochemical quartz crystal microbalance (EQCM), was studied by cyclic voltammetry (CV) and electrochemical quartz crystal microgravimetry. The electrolytic medium employed was a bisulfide-containing aqueous buffered solution (pH 9.2). CV parameters showed that the formation of the Cu_2S phase occurred by means of an irreversible diffusion-controlled mechanism, where a first uncomplicated electron transfer was the rate-determining step. The EQCM data showed that the initially formed phase was Cu_2S, which was later oxidized to nonstoichiometric compounds ($Cu_{(2-x)}S$) and CuS. Furthermore $\Delta Q/\Delta m$ data analysis established that the electron reaction valence (n) was close to 2 for all electrochemical processes where Cu/S compounds were involved. The nucleation and growth mechanism (NGM) of the Cu_2S phase corresponded to a bidimensional instantaneous mechanism containing two contributions, one controlled by diffusion and the other controlled by charge transfer. Atomic force microscopy (AFM) revealed that the Cu_2S phase electroformed on the gold/crystal quartz electrode was deposited as hemispherical particles (sized between 40 and 130 nm) on the terraces and in the cavities present in the gold film.

1. Introduction

Thin films of semiconductors can be considered quasi-bidimensional when the thickness of the film is very small. Normally, they can be considered nanostructured materials, and under such conditions, they represent an alternative approach to efficient and economical solar energy conversion over polycrystalline materials.[1] To obtain a thin film of semiconductor material, the electrodeposition is an excellent technique. At the relatively low temperature of electrodeposition, interdiffusion is not much of a problem, and nanoscale and nanophase materials can be obtained.

Copper sulfide Cu_xS ($x \rightarrow 2$) thin films have received particular attention since the discovery of the CdS/Cu_2S heterojunction solar cell.[2] Moreover, cuprous sulfide is also important in solar technology as a component in the ternary compound semiconductor $CuInS_2$ with an optical band gap of 1.52 eV. This compound provides a good match to the solar spectrum and, unlike its counterpart $CuInSe_2$, does not contain noxious selenium. It is well-known that both natural and synthetic Cu_xS compounds have distinctive compositions because of the variation of the stoichiometric factor (x) ($1 \leq x \leq 2$), where the end members are Cu_2S (chalcosite) and CuS (covellite). Intermediate phases include $Cu_{1.97}S$ (djurleite), $Cu_{1.8}S$ (digenite), and $Cu_{1.4}S$ (anilite), and others have been proposed,[3,4] and their stoichiometry depends on the oxidation degree and temperature.[5−6] These compounds are p-type semiconductors with copper vacancy defects as acceptors. Their distinctive compositions are not significant in the crystalline structure changes, but they are significant in the variation of electrical resistance and in the optical band gap.[3,7] In the heterojunction CdS/Cu_xS solar cell, the magnitude of the short-circuit current is a function of x in the Cu_xS and attains a maximum value at $x = 2$.[8] Among the numerous techniques that have been investigated for producing Cu_xS thin films are vacuum evaporation,[9] chemical bath deposition,[10] successive ionic layer adsorption reaction (SILAR),[11] and so on. For the interest of the present work, special mention of previous research related to the electroformation of Cu_xS will be made. The kinetics and mechanism of Cu_2S film formation on a bare copper electrode as a function of sulfide concentration and pH solution were studied by cyclic voltammetry and transient techniques. It was found that the film grew through a nucleation and growth mechanism that was controlled by localized hemispherical diffusion, which, in the long run, turned into linear diffusion.[12] Potentiostatic current transients applied on copper electrodes in alkaline solution containing Na_2S showed a complex sequence of copper sulfide formation, $Cu_{1.8}S$, CuS, and copper oxide. The instantaneous average anodic currents observed were considered the result of the contributions that supported the formation of these species according to the potential applied.[13] Thin films of $Cu_{(2-x)}S$ and $Cu_{(1+x)}S$ were electrodeposited on different substrates at temperatures that ranged from 21 to 120 °C in a propylene glycol solution of $CuNa_2EDTA$ and sulfur. The stoichiometry and the crystallinity of these compounds depended on the stirring of the solution and on the temperature of the experiments.[14] A study of anodic Cu_xS film, grown by voltammetry combined with electrochemical quartz crystal microgravimetry/coulometry techniques, revealed the initial formation of a Cu_2S phase. Further oxidation resulted in a nonstoichiometric overlayer that ended as a CuS surface.[15] The previously mentioned studies related to the electroformation of a Cu_2S film were carried out mainly by means of the sulfurization of bulk copper electrodes. The present work considered the sulfurization, in an alkaline electrolyte containing sulfide ion, of a thin film of copper deposited onto the gold/crystal quartz electrode of a microelectrochemical balance. A voltammetric/nanoelectro-

* Corresponding author. Fax: +56-32-273422. E-mail: rcordova@ucv.cl.

10.1021/jp026485q CCC: $22.00
Published on Web 11/14/2002

gravimetric study was performed relating the variation of the electrical charge with the mass variation that took place during the process of electroformation of a thin phase of Cu_2S and during its oxidation toward more oxidative species (nonstoichiometric compounds). An *I*/*t* transient study was performed to obtain insight into the nucleation and growth mechanisms of the Cu_2S phase electroformed under the experimental conditions examined. Although the present voltammetric data related to the electroformation of a Cu_2S phase on a thin copper film were not appreciably different from results obtained previously on bulk copper electrodes,[12,13,15] they allowed us to establish a mechanistic sequence for this process, which was not previously reported for studies performed on bulk polycrystalline copper electrodes. On the other hand, our *I*/*t* transient study showed an important difference with respect to similar studies performed on bulk polycrystalline copper electrodes.[12,13] The difference lies principally in the fact that the nucleation and growth mechanism (NGM) of the electroformation of the Cu_2S phase on a thin film of copper takes place through a bidimensional NGM. A similar behavior was observed for a thin film of copper deposited on indium tin oxide (ITO) electrodes.[21] Finally, a morphological study of the Cu_2S phase electroformed on a gold/crystal quartz electrode was carried out by means of atomic force microscopy (AFM).

2. Experimental Section

The electrochemical experiments were performed in a single-compartment three-electrode glass cell. The counter electrode was a platinum wire of wide area (5 cm^2), and the reference electrode was a saturated calomel (0.242 V vs NHE). The gold working electrode was a polycrystalline thin film deposited on a quartz resonator (Si/Au) with a geometric area of 0.20 cm^{-2} (Elchema). An AT-cut quartz crystal resonating at a fundamental frequency of 10 MHz was employed in this study. Before deposition of the copper, the Si/Au system was cleaned with a freshly prepared mixture of H_2SO_4/HNO_3 (1:1) for 2 min, extensively rinsed with milli-Q water, dried with argon, and placed on a spin-coater apparatus. An aliquot (0.3 mL) of the solution of the compound $[CH_3(CH_2)_3CH(C_2H_5)COO]_2Cu{\cdot}2H_2O$ in dichloromethane (5 g L^{-1}) was dispensed onto an exposed face of the Si/Au, and then it was rotated at a speed of 2400 rpm, allowing it to spread. After the spinning was stopped, a thin film of the copper complex remained on the Si/Au. This procedure was applied three times. Later, the exposed face of the Si/Au/Cu complex film system was irradiated with light from a UV lamp (UVP, model UVS-28, 254 nm, 8 W) for 24 h. A film that contained a mixture of copper metal and oxygen-containing copper species was obtained through the photodecomposition of the copper organic complex film.[16] This system consisted of quartz/Au/copper species interfaces and was mounted on the electrochemical cell, exposing the treated surface to the electrolytic solution (0.05 M $Na_2B_4O_7$, pH 9.2). Subsequently, all oxygen-containing copper species present on the electrode surface were reduced by applying a potentiostatic pulse at -1.2 V for 20 min; thus, an electroreduced system was obtained that consisted of quartz/Au/Cu interfaces and will be referred to as a Au/Cu film electrode. Cyclic voltammetry was employed to characterize this Au/Cu film electrode in the potential range from -1.2 to 0 V at a scan rate of 0.02 V s^{-1}. Later, a voltammetric study with the Au/Cu film electrode, in an 0.05 M $Na_2B_4O_7$, pH 9.2, buffer solution containing 60 mM $\geq HS^- \geq$ 4 mM at a scan rate of 0.2 V $s^{-1} \geq \upsilon \geq$ 0.01 V s^{-1} was performed. First, a polarization at -1.2 V was applied for 10 min; then, a sodium sulfide solution was added, and the polarization was maintained for an additional 10 min. Afterward, the potential was stepped to -0.95 V for 5 min while the EQCN instrument was adjusted at a relative mass value of 0. A cyclic voltammetry program was applied starting from that potential. The potential range in the positive-going (forward) potential scan was from -0.95 to -0.6 V, and in the negative-going (reverse) potential scan, it was from -0.6 to -1.2 V. Potentiostatic current transients studies with the Au/Cu film electrode were performed in a 0.05 M $Na_2B_4O_7$ buffer solution containing 5 mM HS^-. The *E*/*t* program applied considered a first potential step at -1.2 V for 10 min, and during this polarization, sodium sulfide was added. Further potential steps were applied in the potential range between -0.90 and -0.76 V, and therefore, thin films of Cu_xS ($x \rightarrow 2$) were obtained. All electrochemical and nanoelectrogravimetric experiments were performed with a Pine potentiostat (Pine Instrument Company, model RDE4) connected to an electrochemical quartz nanobalance (Elchema, EQCN-501). The experiments were carried out at ambient temperature (18−20 °C) under argon atmosphere. Analytical-grade reagents and freshly made sodium sulfur solutions were employed. Morphology studies of Si/Au and sulfurized Au/Cu film electrode were performed ex situ with a Nanoscope llla (Digital Instruments, Santa Barbara, CA) in tapping and contact modes. All deconvoluted *I*/*E* and *I*/*t* profiles presented in this work were obtained by applying a nonlinear curve-fitting program (Microcal Origin 5.0).

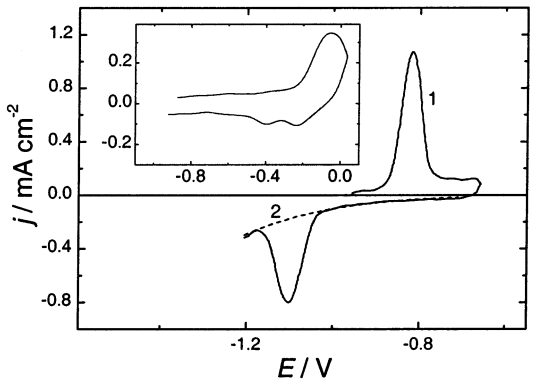

Figure 1. Cyclic voltammograms of a Au/Cu film electrode in 0.05 M $Na_2B_4O_7$, pH 9.2, at a scan rate of 0.02 V s^{-1}: (1) in the presence of 5 mM Na_2S, (2) water electroreduction *I*/*E* profile (dashed line). The inset shows the CV of a Au/Cu film electrode in the absence of sulfide ion.

3. Results and Discussion

3.1. Voltammetry. Figure 1 shows the voltammetric profiles of a Au/Cu film electrode in a 0.05 M $Na_2B_4O_7$ buffer solution, pH 9.2, both in the presence and in the absence of sodium sulfide. For the Au/Cu film electrode in the absence of sulfide ion, the voltammetric profile shows a broad anodic current maximum located at a potential of -0.05 V that follows a prepeak located close to -0.4 V. Those processes are related to the formation of cuprous oxide. In the reverse potential scan, at least two peaks are clearly observed at potentials of -0.23 and -0.4 V, which corresponds to the reduction of cuprous oxide. The charge ratio Q_a/Q_c is close to unity. The anodic and cathodic processes described above are in accordance with previously reported results corresponding to the behavior of copper electrodes in alkaline media.[12,15,17]

In the presence of 5 mM HS^-, only a well-defined anodic current peak is observed at -0.82 V, which is attributed to the Cu_xS electroformation. Under the experimental conditions employed, the underpotential deposition (UPD) of a hydrosulfide

layer on the copper surface is not observed, although it has been described by other authors.[15] In the reverse potential scan starting at −0.65 V, only a cathodic maximum current peak located at −1.10 V is observed; it corresponds to cuprous sulfide reduction and appears superimposed on the water discharge reaction profile (dashed line), which was obtained by deconvolution of the whole cathodic profile. The process of electroformation of the Cu_xS phase appears electrochemically irreversible, and the Q_a/Q_c charge ratio corresponding to the first potentiodynamic cycle was close to 0.96. This value reflects the fact that the reduction of copper sulfide formed via electrochemical and chemical processes takes place during the reverse potential scan, with the latter process occurring through a parallel pathway. Although the spontaneous formation of Cu_2S was previously described by other authors,[15] its origin was not established at that time. In this work, this process has been attributed to the occurrence of the reaction

$$2Cu + H_2O + HS^- \rightarrow Cu_2S + OH^- + H_2 \qquad (1)$$
$$\Delta G^\circ = -18.9 \text{ kJ}$$

The above reaction is assumed because the electroreduction of water is always present in the potential range assayed and the global process would be considered as a corrosion process. Figure 2 shows the potentiodynamic parameters that characterize the electroformation of a thin layer of Cu_xS ($x \rightarrow 2$) on a Au/Cu film electrode. Figure 2A shows linear relationships of the logarithm of the current density (log j) and the anodic current peak potential (E_p) with the sulfide concentration. The slopes were close to 1 and 2.303RT/F, respectively. These values reveal that a first-order reaction for sulfide ion concentration ocurs and that the electrode process shows Nernstian behavior. Figure 2B shows a plot of E_p versus the logarithm of the scan rate (υ). A slope value $\partial E_p/\partial(\log \upsilon)$ close to $1.15RT/\alpha_a F$ is obtained[18] (−59 mV, considering an anodic transfer coefficient $\alpha_a = 0.5$), indicating that the rate-determining step (rds) in the sulfurization process corresponds to the first electron transfer. Figure 2 C shows a plot of the logarithm of j_p versus the logarithm of υ. A slope $\partial(\log j_p)/\partial(\log \upsilon)$ close to 0.5 indicates the existence of a diffusion-controlled electrochemical process. In the same figure, a constant value for the logarithm of the peak current function [$\log(j_p\upsilon^{-1/2}) = -2.08$] versus the logarithm of υ shows that Cu_xS ($x \rightarrow 2$) formation takes place through an uncomplicated totally irreversible charge-transfer reaction.[19] From this constant value, a diffusion coefficient value (D_0) close to 1.5×10^{-5} cm^2 s^{-1} was estimated for HS^- ion by the equation

$$\log(j_p\upsilon^{-1/2}) = \log(2.99 \times 10^5 n\alpha_a^{1/2} C_0 D_0^{1/2}) \qquad (2)$$

where $n = 2$, $\alpha_a = 0.5$, and C_0 is the sulfide ion concentration (5×10^{-6} mol cm^{-3}).

Considering all of the above potentiodynamic parameters and previously reported results,[15,20] the following reaction sequence is proposed.

SCHEME 1: Reaction Sequence for the Electroformation of a Cu_2S Phase

$$2Cu + HS^- \rightarrow Cu_2(HS)_{ad}^- \qquad (3)$$

$$Cu_2(HS)_{ad}^- \xrightarrow{\text{rds}} Cu_2(HS)_{ad} + e^- \qquad (4)$$

$$Cu_2(HS)_{ad} \rightarrow Cu_2S + H^+ + e^- \qquad (5)$$

3.2. Electrochemical Quartz Crystal Nanogravimetry/Coulometry. *3.2.1. Stoichiometric Compound.* Figure 3 shows the *I*/*E* potentiodynamic profile starting at −0.95 V corresponding to the anodic electroformation of Cu_2S ($Q_a = 0.625$ mC) and its respective electroreduction ($Q_c = 0.651$ mC). The simultaneous mass variation registered during the *I*/*E* profile is also shown. In the forward potential scan, from the initial potential, the mass decreases, attaining a value close to −20 ng (Δm_1). This initial mass decrease was also observed by de

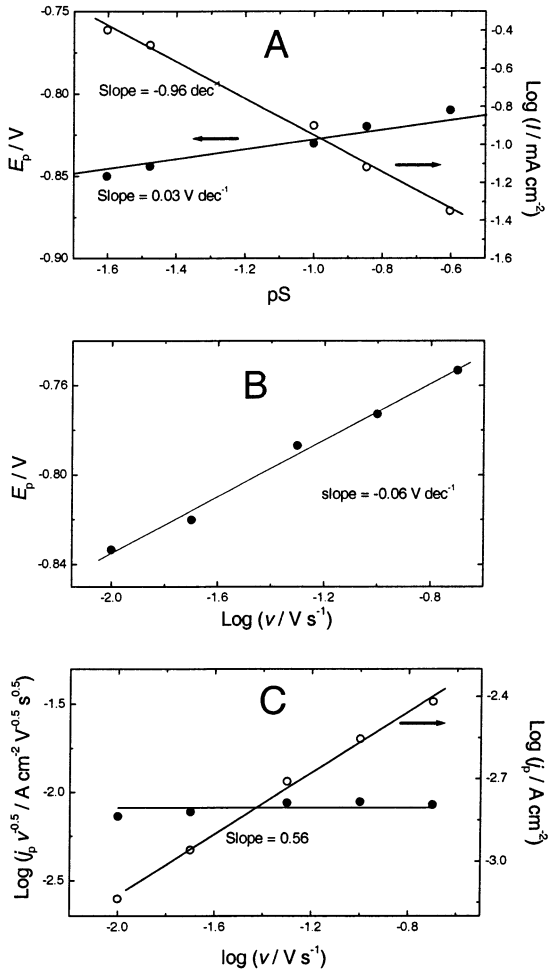

Figure 2. Potentiodynamic parameters related to Cu_2S formation: (a) peak potential variation and log j as a function of the logarithm of the sulfide molar concentration, (b) peak potential variation as a function of the logarithm scan rate, (c) variation of the logarithm of the anodic current peak and log $j_p\upsilon^{-1/2}$ as a function of the scan rate.

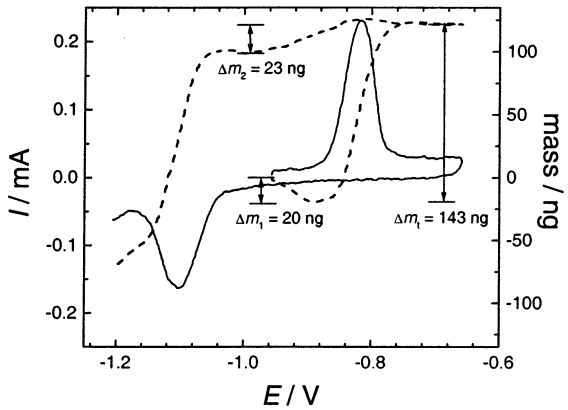

Figure 3. *I*/*E* (solid line) and *m*/*E* (dashed line) potentiodynamic profiles for a Au/Cu film electrode in 0.05 M $Na_2B_4O_7$, pH 9.2, 5 mM Na_2S, at a scan rate of 0.02 V s^{-1}. Δm_t, total mass variation; Δm_1, mass variation due to copper electrodissolution (eq 6); Δm_2, mass variation attributed to desorption of species (see text).

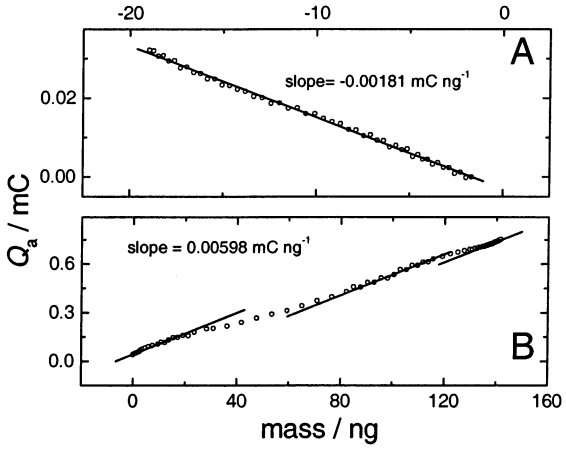

Figure 4. Q vs m plots for different potential ranges: (A) -0.95 to -0.90 V, (B) -0.9 to -0.75 V (data obtained from Figure 3).

Tacconi et al.[15] and was attributed to the incipient electrodissolution of copper from the electrode expressed by the equation

$$Cu_2(HS)_{ads}^{-} \rightarrow 2Cu^{+} + HS^{-} + 2e^{-} \qquad (6)$$

This process continues until the cuprous and sulfide ion concentrations present at the interface result in an ionic product value ($[Cu^{+}]^2[S^{2-}]$) greater than the constant solubility product of Cu_2S ($K_{ps} = 3 \times 10^{-49}$). At this moment, the copper deposits back onto the electrode surface as cuprous sulfide. From the minimal mass value, the mass increases monotonically until it reaches a constant value close to 123 ng related to the growth of the copper sulfide layer through the sequence of reactions shown in Scheme 1. Because copper is present in the electrode, most of the net mass change ($\Delta m_t = 143$ ng) corresponds to the sulfur entering the film (vide infra).

In the reverse potential scan registered from -0.65 to -0.98 V, the mass decreases by 23 ng (Δm_2). This mass decrease is not related to an electrochemical process associated with the electroreduction of the Cu_2S phase, and it could correspond to the desorption of species incorporated during the forward potential scan, together with the entering of sulfur into the film. In the potential range from -0.95 to -1.2 V, the mass decreases concomitantly with the electroreduction of the Cu_2S formed. The final mass value attained was negative ($m = -69$ ng) with respect to the initial value ($m = 0$). This result was attributed to the different interfacial compositions that were attained at both potentials, but principally to the reduction of the Cu_2S chemically formed at the initial potential (-0.95 V).

Figure 4 shows the variation of the anodic electrical charge (Q_a) with the mass (m). The data were obtained from Figure 3 in the potential range from -0.95 to -0.75 V. Figure 4A corresponds to the potential region where a mass decrease and a linear relationship with a slope of $\Delta Q/\Delta m = 1.81 \times 10^{-3}$ mC ng^{-1} are observed. From this value slope, using the equation[15]

$$n = \frac{\Delta Q_a}{\Delta m}\left(\frac{M_{Cu}}{F}\right) \quad \text{with} \quad \left(\frac{M_{Cu}}{F}\right) = 658 \text{ ng mC}^{-1} \qquad (7)$$

where M_{Cu} is the molar mass of copper and F is the faraday constant, an electrode reaction valence (n) of 1 ± 0.2 was obtained. This value is consistent with the initial copper electrodissolution step expressed by eq 6. On the other hand, Figure 4B shows a plot of Q_a/m for the potential range from -0.9 to -0.75 V. Three regions with linear relationships with slopes of $\Delta Q/\Delta m = 5.98 \times 10^{-3}$ mC ng^{-1} appear clearly defined. By means of the equation[15]

$$n = \frac{\Delta Q_a}{\Delta m}\left(\frac{M_S}{F}\right) \quad \text{with} \quad \left(\frac{M_S}{F}\right) = 332 \text{ ng mC}^{-1} \qquad (8)$$

where M_S is the molar mass of sulfur, an electrode reaction valence (n) value of 1.99 ± 0.01 was obtained. This value is consistent with a sulfurization process of copper represented by the reaction sequence shown in Scheme 1.

The existence of three parallel linear relationships in Figure 4B indicates that, in the discontinuity regions of the plot, the mass detected is greater than what would correspond to the net Cu_2S electroformation process. This fact is attributed to the simultaneous adsorption of species coming from the electrolyte and also to a chemical Cu_2S formation process that takes place simultaneously with the electrochemical one. The chemical process should contribute with ca. 4.3 ng (Δm_3), taking into account that the experimental Q_a/Q_c ratio is 0.96. A mass balance that considers all occurring processes is as follows: the total mass change ($\Delta m_t = 143$ ng) includes the mass of copper redeposited as Cu_2S ($\Delta m_1 = 20$ ng), the mass of adsorbed species ($\Delta m_2 = 23$ ng), the mass of sulfur in Cu_2S chemically formed ($\Delta m_3 = 4.3$ ng), and the mass of sulfur in the Cu_2S electroformed (Δm_4). From the above figures, a value of 95.7 ng is estimated for Δm_4. By relating this Δm_4 value to the measured electrical anodic charge (0.625 mC), an electrode reaction valence value (n) of 2.2 ± 0.2 was obtained through eq 8. This value is in accordance with the sulfurization process of copper represented by Scheme 1.

3.2.2. Nonstoichiometric Compound. The formation of nonstoichiometric copper sulfide intermediates during the electrochemical oxidation of natural and synthetic chalcocite in aqueous media was previously proposed.[3,4] Figure 5A shows the potentiodynamic I/E profile starting at -0.90 V, which presents an anodic current peak located at -0.82 V (0.478 mC) that precedes a complex anodic current contribution. The anodic current peak corresponds to the electroformation of Cu_2S, and the complex anodic current contribution would correspond to the electrooxidation of Cu_2S toward nonstoichiometric compounds represented by $Cu_{(2-x)}S$ ($1 \geq x$) and to the electrooxidation of HS^{-} ions toward sulfur and polysulfide species (S_n^{2-}) (vide infra). These two last processes are thermodynamically possible in the potential range and pH range investigated.[21,22] In the reverse scan registered in the potential range from -0.47 to -1.2 V, two complex cathodic current peak located at -0.66 and -0.82 V were observed before a well-defined cathodic current peak located at -1.12 V (0.522 mC) developed. The last past is due to the electroreduction of Cu_2S, and the complex cathodic current contributions include the electroreduction of nonstoichiometric copper sulfide compounds, elemental sulfur, and S_n^{2-} species. It is important to mention that the appearance of one or two cathodic current peaks in the complex cathodic current contributions is strongly dependent on the anodic potential switch considered. The Δm variation that takes place simultaneously during the register of the potentiodynamic I/E profile is also shown.

In the forward potential scan, the mass increases continuously, and five steps are evidenced, showing the complexity of the electrochemical processes that are occurring and that involve the arrival of sulfur at the film and the absorption of species coming from the solution. In the reverse potential scan, initially, the mass increases until it attains a maximum value, and then a mass variation is observed, where decreasing and increasing steps alternate along most of the m/E profile. This behavior has

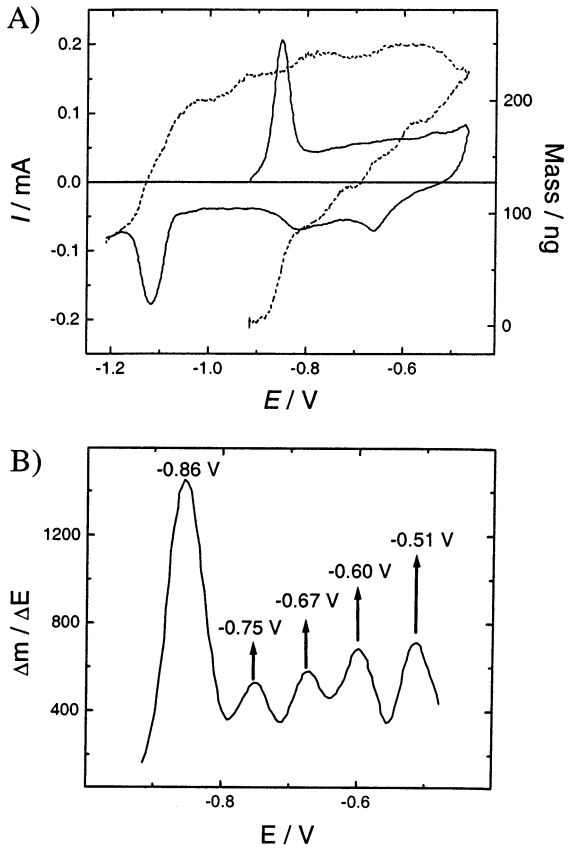

Figure 5. (A) *I*/*E* (solid line) and *m*/*E* (dashed line) potentiodynamic profiles for a Au/Cu film electrode in 0.05 M $Na_2B_4O_7$ pH 9.2, 5 mM Na_2S, at a scan rate of 0.02 V s^{-1}. (B) $\Delta m/\Delta E$ vs *E* plot for the anodic *m*/*E* profile.

TABLE 1: Electrical Charge Associated with Anodic and Cathodic Current Contributions from Figure 6

anodic current contribution	Q_a (mC)	cathodic current contribution	Q_c (mC)	Q_a/Q_c	electrochemical process assigned
A_1	0.478	C_1	0.522	0.92	9
A_2	0.103	C_2	0.102	1.01	10
A_3	0.153	C_3	0.162	0.94	11
A_4	0.210	C_4	0.204	1.03	12
A_5	0.165	C_5	0.172	0.96	13
A_6	0.385	C_6	0.277	1.39	14
		C_7	0.542		15

been attributed to the adsorption of species that occurs simultaneously with the departure of sulfur as a consequence of the electroreduction of the elemental sulfur and nonstoichiometric copper sulfide compounds. The final mass value attained is higher than the initial mass value ($m = 0$), which means that the species adsorbed during the anodic and cathodic voltammetric scan remain on the working electrode at the final potential. The possibility that nonstoichiometric compounds not completely reduced in the reverse potential scan would remain on the electrode is rejected, because the charge ratio (Q_a/Q_c) obtained from the respective anodic and cathodic voltammetric profiles is close to 1 (see Table 1). A $\Delta m/\Delta E$ vs *E* plot (Figure 5B) for the anodic *m*/*E* profile reveals five peaks located at the potentials indicated in the figure corresponding to the electrochemical processes responsible for the mass variation. The first is attributed to the electroformation of the Cu_2S phase, and the others could be associated with the formation of nonstoichiometric compounds and elemental sulfur.

To obtain insight the anodic and cathodic electrochemical processes described above, deconvolutions of the respective *I*/*E* profiles were performed (Figure 6). Because the anodic profile appears not adequately featured, the respective deconvolution considered the potentials values of the peaks indicated in Figure 5B. It is observed that for the anodic and cathodic profile, the fittings closely follow the experimental data. Figure 6A shows the deconvoluted anodic profile, which considers five anodic current peak contributions located at −0.85 V (A_1), −0.76 V (A_2), −0.70 V (A_3), −0.63 V (A_4), and −0.54 V (A_5). These are attributed to the electroformation of the Cu_2S phase (A_1)

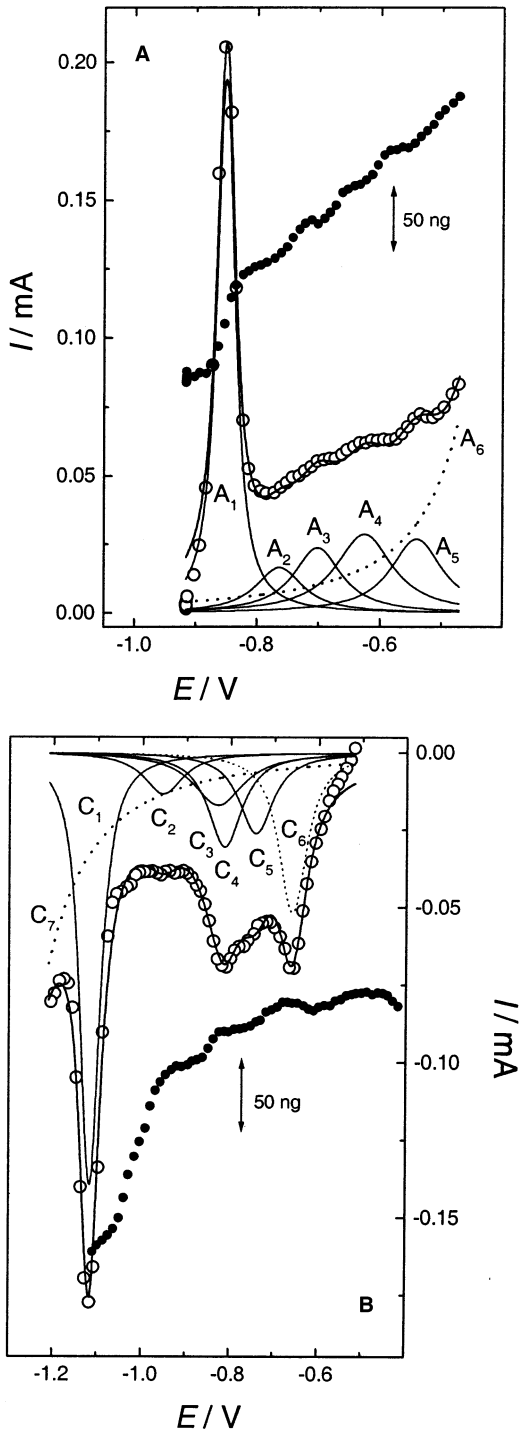

Figure 6. *m*/*E* profile and deconvoluted *I*/*E* profile for a Au/Cu film electrode in 0.05 M $Na_2B_4O_7$, pH 9.2, 5 mM Na_2S, at a scan rate of 0.02 V s^{-1}: (A) anodic profiles, (B) cathodic profiles. Experimental *m*/*E* data (solid circles), experimental *I*/*E* data (open circles), fitted *I*/*E* data (solid line). A_1, A_2, A_3, A_4, A_5, and A_6, anodic current contributions; C_1, C_2, C_3, C_4, C_5, C_6, and C_7, cathodic current contributions.

and to the formation of nonstoichiometric compounds (A_2, A_3, A_4) obtained from the oxidation of the Cu_2S phase. The contributions A_5 and A_6 are attributed to the oxidation of HS^- to elemental sulfur and S_n^{2-} species, respectively. The electrochemical processes denoted as A_1, A_2, A_3, A_4, and A_5 are related to the mass variation observed in the *m*/*E* profile, and their respective potentials are located close to the potential values of the peaks shown in Figure 5B. Furthermore, the electrooxidation of HS^- to S_n^{2-} species (A_6) is present throughout the potential range (dashed line) and precedes the sulfur electroformation (A_5). The former process (A_6) is not related to the mass changes, because the electroformed S_n^{2-} species diffuse away from the electrode surface.

Figure 6B shows the cathodic deconvoluted profile, where six cathodic current peak contributions are considered. They are located at −0.66 V (C_6), −0.74 V (C_5), −0.81 V (C_4), −0.84 V (C_3), −0.95 V (C_2), and −1.12 V (C_1), and an exponential cathodic current contribution (C_7) is also present. The contributions C_6 and C_5 are attributed to the electroreduction of elemental sulfur and S_n^{2-} species; C_4, C_3, and C_2 to the electroreduction of different nonstoichiometric compounds; and C_1 to the electroreduction of the Cu_2S phase. The cathodic contribution C_7 is attributed to the electroreduction of water, which occurs throughout the potential range of the negative scan. The electrical charges associated with each contribution present in the anodic and cathodic profiles are summarized in Table 1. It is observed that the ratio Q_a/Q_c for each couple of anodic and cathodic processes is close to 1, except for the ratio Q_a/Q_c that is attributed to the electroformation and electroreduction of S_n^{2-} species. In this case, the S_n^{2-} ions formed would remain partially in the interface, and only a fraction of them could be reduced in the reverse scan.

According to the data summarized in Table 1, the following electrochemical reactions (eqs 9−15) are proposed

$$2Cu + HS^- \leftrightarrow Cu_2S + H^+ + 2e^- \quad (9)$$

$$Cu_2S + xHS^- \leftrightarrow Cu_{2-x}S{\cdot}xCuS + xH^+ + 2xe^- \quad (10)$$

$$Cu_{2-x}S{\cdot}xCuS + yHS^- \leftrightarrow Cu_{2-x-y}S{\cdot}(x+y)CuS + yH^+ + 2ye^- \quad (11)$$

$$Cu_{2-x-y}S{\cdot}(x+y)CuS + zHS^- \leftrightarrow 2CuS + zH^+ + 2ze^- \qquad x + y + z = 1 \quad (12)$$

$$HS^- \leftrightarrow S + H^+ + 2e^- \quad (13)$$

$$nHS^- \leftrightarrow S_n^{2-} + nH^+ + 2(n-1)e^- \quad (14)$$

$$2H_2O + 2e^- \rightarrow H_2 + 2OH^- \quad (15)$$

Through eq 16, a relationship was made between the anodic charges A_2, A_3, and A_4 and the charge A_1, which is associated with the formation of Cu_2S. Considering the respective charge values of Table 1, an estimation of the stoichiometric factor (x) present in the Cu_xS compounds was made through eq 16, and therefore, the nonstoichiometric compounds that could be formed by means of the oxidation of Cu_2S could be $Cu_{1.8}S$ (A_2), $Cu_{1.5}S$ (A_3), and CuS (A_4)

$$x = 2 - \left(\frac{\sum_2^n Q_n}{Q_1}\right) \quad \text{where} \quad n = 2, 3, 4 \quad (16)$$

To confirm the reactions proposed above, charge/mass relationships were established from the *I*/*E* and *m*/*E* anodic and cathodic profiles (Figure 7). Previously, the current contributions that did not produce a mass variation were subtracted from the respective original *I*/*E* profile. Figure 7A represents the anodic charge versus mass variation without the contribution of the process A_6 (dotted line in Figure 6A), and a linear relationship with a slope value of 0.0054 mC ng^{-1} is obtained. Taking into account that all of the anodic processes that favor Cu/S compounds formation involve the entrance of sulfur into the electrode film, an n value of 1.8 ± 0.1 for the electrode reaction valence was determined by means of eq 8. This value is close to the expected one ($n = 2$) for the electrochemical processes represented by the reactions in eqs 9−13.

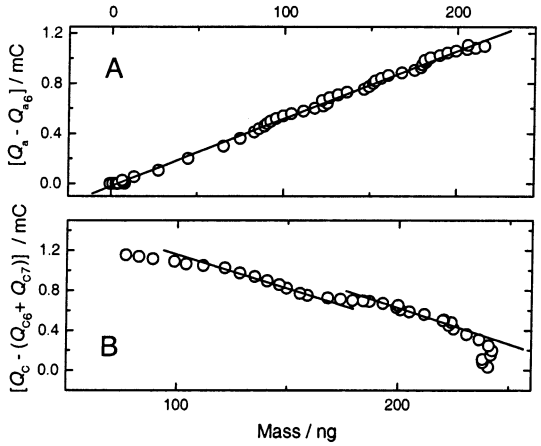

Figure 7. Plot of Q vs mass change obtained from Figure 6 by subtraction in (A) anodic contribution A_6 and (B) cathodic contributions C_6 and C_7.

Similarly, to obtain the respective $Q_c/\Delta m$ plot for the cathodic processes, the original cathodic *I*/*E* profile was corrected by subtracting from it the current contributions of C_6 and C_7 (dotted lines in Figure 6B). Figure 7B shows a $Q_c/\Delta m$ plot for the corrected *I*/*E* profile and two parallel linear relationships with a slope value of 0.0057 mC ng^{-1}. This figure allows for the calculation of an electrode reaction valence (n) of 1.9 ± 0.1; this value arises because sulfur leaves the electrode surface during the electroreduction processes. Moreover, two other regions are observed in the plot where the mass varies above the expected value. This behavior can be related to the adsorption on the electrode of species that come from the solution. For potentials more positive than −0.80 V (see Figure 5A), the mass remains almost constant. This fact is not in accordance with the cathodic electrochemical processes (eqs 12 and 13) where a mass decrease due to the departure of sulfur is expected, and it is attributed to the adsorption of species that compensate the mass decrease expected for the electroreduction processes.

3.3. Nucleation and Growth Mechanism Studies for the Formation of a Cu_2S Phase. Figure 8 shows various *I*/*t* experimental transients obtained by holding the initial potential of the Au/Cu film electrode at −1.20 V for 20 min and then stepping to a final potential E_s of between −0.90 and −0.75 V in a 0.05 M $Na_2B_4O_7$, pH 9.2, 5 mM Na_2S electrolytic solution. The general shape of the *I*/*t* transient is characteristic of a nucleation and growth process. At very short times (t < 1 s), double-layer charging occurs, and then the current increases as a result of the formation and growth of the Cu_2S nuclei. The current rises until it reaches a maximum value, and finally, it decreases to a stationary negative current value at times longer than 30 s (not shown in the Figure 8).

Stationary negative current values were observed for all potentials studied, and this phenomenon was attributed to the

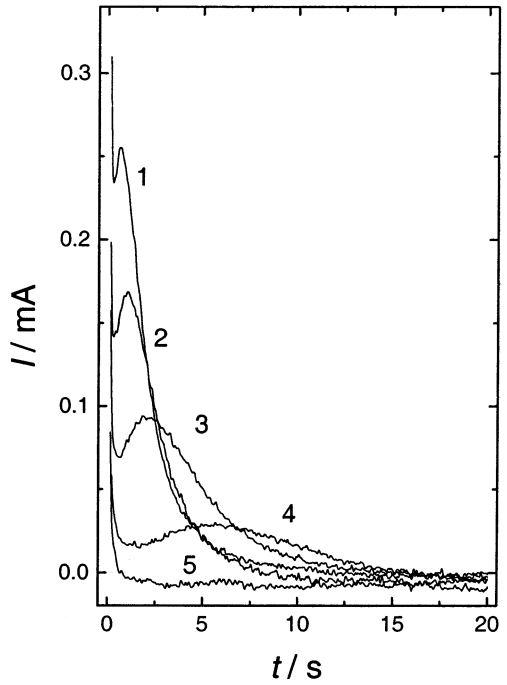

Figure 8. $I-t$ transients of a Au/Cu film electrode at constant potentials in 0.05 M $Na_2B_4O_7$, pH 9.2, 5 mM Na_2S solution: (1) −0.81, (2) −0.83, (3) −0.85, (4) −0.87, and (5) −0.89 V.

water reduction that occurred simultaneously with the electroformation of the Cu_2S film. This behavior was identical to the sulfurization process that takes place on nanostructured cooper deposits on ITO electrode[20] and is observed only when thin copper films with a limited number copper sites available for sulfurization are employed as the substrate. In fact, when $I-t$ transients were obtained under identical experimental conditions using bulk mirror-polished copper electrodes, the stationary currents observed were positive, in accordance with previously reported results.[12,13] In this case, the positive stationary current observed was the result of the continuous anodic growth of the Cu_2S film (majority process) and the electroreduction of water (minority process).

Therefore, to obtain corrected $I-t$ transients of the electroformation of Cu_2S on thin copper films, eq 17 was employed to subtract from the $I-t$ transients the current contribution attributed to water reduction

$$I = -a[1 - \exp(-bt^2)] \tag{17}$$

This equation was postulated considering that water reduction takes place simultaneously with electroformation of the Cu_2S phase and follows an exponential law. Under this assumption, a constant current value was attained as $t \rightarrow \infty$. In the expression above, I is the current related to water reduction, t is the time considered, a and b are constants that depend on the potential value applied. Both constants were evaluated by a nonlinear fit procedure. The corrected $I-t$ transients are represented in a dimensionless plot (Figure 9) for an evaluation of the type of nucleation and growth mechanism (NGM) of the Cu_2S phase. Thus, calculating the dimensionless parameters I/I_m and t/t_m, where I is the transient current at a t time and I_m and t_m are the current and time values, respectively, corresponding to the maximum of the $I-t$ transient. It was established that the NGM is instantaneous bidimensional (IN2D) through a comparison of the experimental plots with the theoretical ones for the two bidimensional limiting nucleation cases, i.e., progressive and instantaneous. This behavior (IN2D) is expected because the

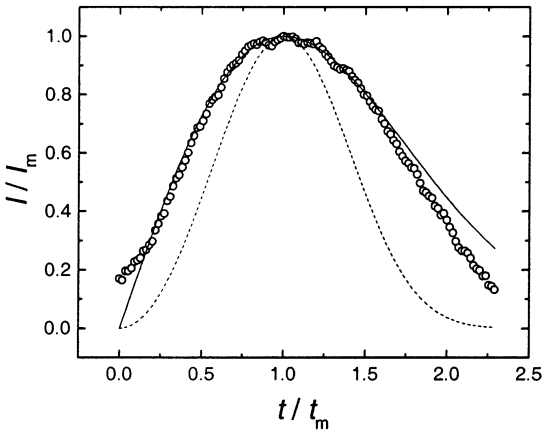

Figure 9. Nondimensional plot for the 2D nucleation of Cu_xS phase on a Au/Cu film electrode obtained from the I/t transient at −0.870 V. Instantaneous nucleation (solid line), progressive nucleation (dotted line), experimental data (open circles).

number of copper sites available for sulfurization is limited and, as a consequence, the current due to Cu_2S electroformation attains a zero value at long times, once all copper sites have reacted. This result was different from that previously reported for bulk mirror-polished copper electrodes,[13] where progressive nucleation with tridimensional growth under diffusion control takes place.

On the other hand, the $I-t$ transients were considered as the sum of three partial current contributions: double-layer charging (I_{DL}) and two contributions (I_I and I_{II}) due to the electroformation of Cu_2S. The contribution I_{DL} is given by

$$I_{DL} = A \exp\left(-\frac{t}{B}\right) \tag{18}$$

where $A = \Delta V/R$ and $B = RC$. ΔV is the amplitude of the potential step, R is the resistance of the interface electrode/electrolyte, and C represents the capacity of the interface.[23]

I_I represents a transient current contribution that corresponds to a process of instantaneous nucleation with circular bidimensional growth under diffusional control.[24] The instantaneous value of I_I is given by

$$I_I = E \exp(-Gt) \tag{19}$$

where $E = q\Pi k_e D N_0$ and $G = \Pi k_e D N_0$. D is the diffusion coefficient of the reacting species (HS^-), k_e is a proportionality constant controlled by the potential, N_0 is the number of cluster sites available for nucleation on the surface, and q represents the charge density required for the sulfurization of the copper sites.

I_{II} represents the current transient contribution associated with an instantaneous bidimensional nucleation process under activated control[25] and obeys the equation

$$I_{II} = Ht \exp(-Lt^2) \tag{20}$$

where $H = 2\Pi FMhN_0K\rho^{-1}$ and $L = \Pi N_0 K^2 M^2 \rho^{-2}$. F is the Faraday constant; M is the molecular weight; N_0 and h are the number and height of the copper cluster, respectively; K is the rate of this nucleation process; and ρ is the density of Cu_2S. Figure 10 (A and B) shows the corrected $I-t$ transients and the respective partial contributions. It is possible to observe that the sum of the deconvoluted contributions reproduces the experimental $I-t$ transients adequately.

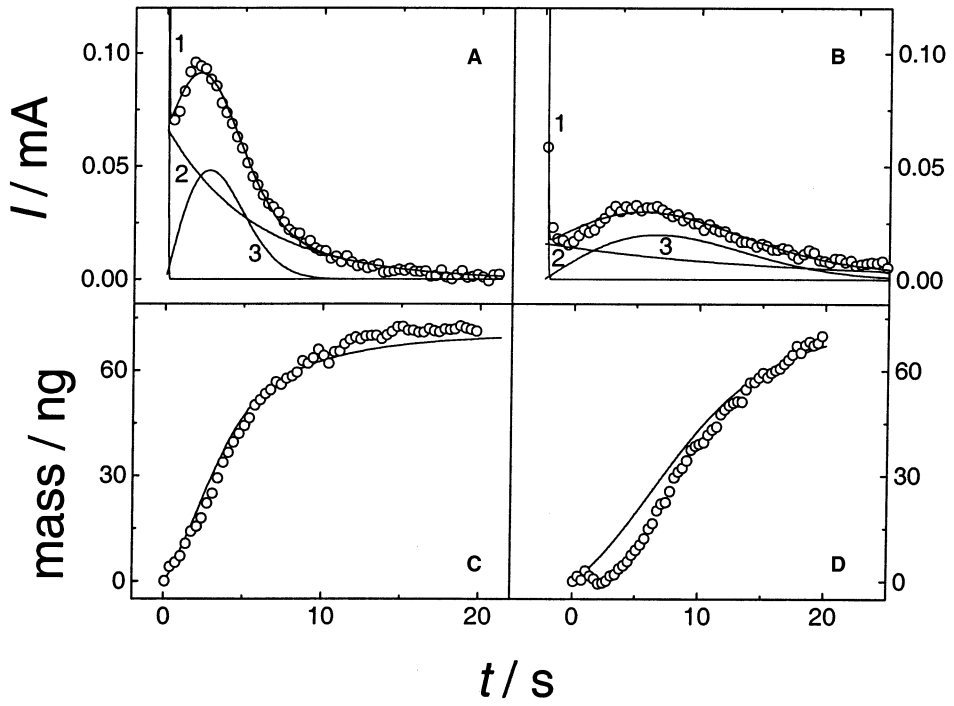

Figure 10. $I-t$ transients obtained with a Au/Cu film electrode in 0.05 M $Na_2B_4O_7$, pH 9.2, 5 mM Na_2S at the potentials (A) −0.85 and (B) −0.87 V. Experimental data (open circles), fitted curve (solid line), individual current contributions (1) I_{DL}, (2) I_I, (3) I_{II}. Mass variation as function of time at (C) −0.85 and (D) −0.87 V. Experimental data (open circles), mass data calculated from Faraday law (solid line).

The presence of two types of nucleation and growth mechanisms (I_I and I_{II}) in the transients consider a substrate model that has two different sites of copper for the sulfurization process. The first holds adsorbed hydrosulfide ions and is responsible for the IN2D process under activated control (I_{II}). The second, without adsorbed hydrosulfide ions, is affected by the diffusion of the hydrosulfide ions from the solution and is responsible for the IN2D process under diffusional control (I_I). Nevertheless, the possibility that the presence of copper on two different sites (terraces and cavities) of the gold film could be responsible for either current contribution is not rejected. The presence of these copper sites is shown in the morphological study of Si/Au and a sulfurized Au/Cu film electrode (vide infra).

This hypothesis was also employed to explain the performance of the $j-t$ transients obtained for the same system on an ITO/Cu substrate.[20]

Figure 10 (C and D) shows the mass variation along the period of time associated with the potentiostatic $I-t$ transients measured at −0.85 and −0.87 V. The experimental mass data (open circles) is compared with the values deduced from the electrical charge at each t time by applying the Faraday law (solid line). Considering that the sulfurization process, represented by eq 21, occurs on a hydrated Au/Cu film electrode, the mass variation with time considers that Γ water molecules are removed from the electrode when a sulfur atom is added as Cu_2S onto the Au/Cu film electrode

$$\text{quartz/Au/2Cu}(H_2O)_n + HS^- \rightarrow$$
$$\text{quartz/Au/Cu}_2\text{S}\cdot(2n-\Gamma)H_2O + H^+ + \Gamma H_2O + 2e^- \quad (21)$$

Consequently, the Faraday law applied can be expressed as follows

$$\Delta m = \left(\frac{\Delta Q}{2F}\right)Z \quad (22)$$

where

$$Z = (M_S - \Gamma M_{H_2O}) \quad (23)$$

In eq 23, M_S and M_{H_2O} represent the molar masses of sulfur and water, respectively, and the Γ value considered is 0 for the polarization at −0.87 V and 0.5 for the polarization at −0.85 V. This means that, when the potential value applied to the electrode becomes more negative, a minor disturbance in the arrangement of water around the electrode is produced when a sulfur atom is added. This effect also occurred when cyclic voltammetry was performed on the system at a relative low scan rate (0.02 V s^{-1}).

3.4. Morphologic Study of Si/Au and Sulfurized Au/Cu Film Electrodes. To study the morphology of Si/Au and a sulfurized Au/Cu film electrode, 3D AFM images of these electrodes were obtained, and they are shown in Figure 11. Figure 11A shows the morphology of the surface of Si/Au, where a flat surface and the wall of a neighbor terrace are observed and a clearly defined furrow appears. From Figure 11A, a height difference close to 200 nm between the two terraces can be estimated. Figure 11B shows the surface of a sulfurized Au/Cu film electrode where hemispherical Cu_2S particles with different sizes (from 40 to 130 nm) are observed on the gold surface. These Cu_2S particles modify the previous topography of the Si/Au. This 3D AFM image shows that the particles of Cu_2S in the sulfurized Au/Cu film electrode were formed on the whole surface of the gold film, covering terraces and cavities. Taking this fact into account, it is possible to consider that the origin of the two types of NGM for the electroformation of a Cu_2S phase could be also due to the existence of two different copper sites. These are located in Au/Cu film electrode on the terraces and in the cavities of the gold film, as observed in Figure 12.

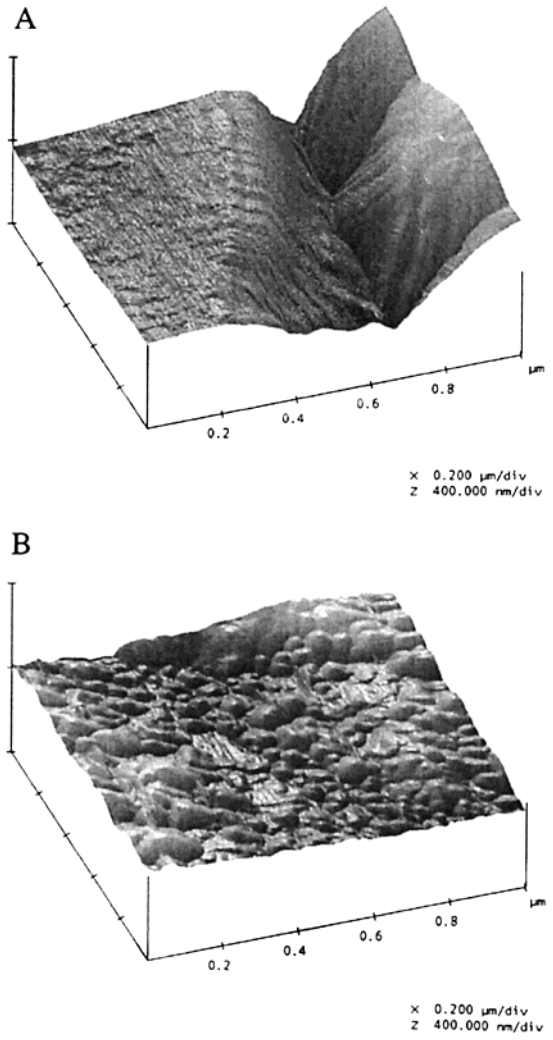

Figure 11. AFM contact-mode images of (A) Si/Au and (B) a Au/Cu film electrode sulfurized by polarization at −0.87 V for 5 min in 0.05 M $Na_2B_4O_7$, pH 9.2, 5 mM Na_2S electrolytic solution.

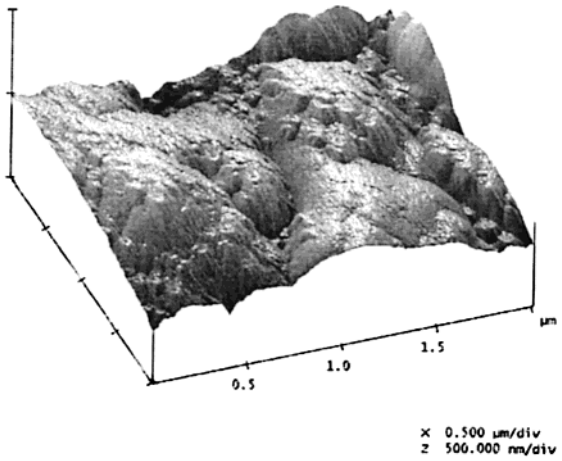

Figure 12. AFM tapping-mode image of Au/Cu film electrode.

4. Conclusions

Cyclic voltammetry parameters showed that the formation of a Cu_2S phase on a Au/Cu film electrode occurred through an irreversible diffusion-controlled mechanism with a first uncomplicated electron transfer as the rate-determining step.

The EQCN data showed that the phase initially formed was Cu_2S.

Charge data analysis allowed us to establish that the non-stoichiometric compounds resulting from the oxidation of the Cu_2S phase were $Cu_{1.8}S$, $Cu_{1.4}S$, and CuS.

All electrochemical processes that involved Cu/S compounds had an electron reaction valence (n) close to 2.

The NGM of the Cu_2S phase corresponded to a bidimensional instantaneous mechanism containing two contributions, one controlled by diffusion and the other controlled by charge transfer.

The AFM study revealed that the deposit of a Cu_2S phase on a sulfurized Au/Cu film electrode modified the topography of the gold surface considerably. Hemispherical Cu_2S particles appeared located both on the terraces and in the cavities of the gold film.

Acknowledgment. We gratefully acknowledge financial support from FONDECYT-Chile (Projects L.C. 8000022 and 3010016) and DGI-UCV (Project 125720/2000). D.B. acknowledges the fellowship granted by FONDECYT.

References and Notes

(1) Meyers, G. J.; Searson, P. C. *Interface* **1993**, *2*, 23.
(2) Reynolds, D. C.; Leiss, G.; Anter, L. T.; Margurber, R. E. *Phys. Rev.* **1954**, *96*, 535.
(3) Koch, D. F. A.; McIntyre, R. J. *J. Electroanal. Chem.* **1976**, *71*, 285.
(4) Young, C. A.; Woods, R.; Yoon, H. In *Electrochemistry in Mineral and Metal Processing II PV 88−21*; Richardson, P. E., Woods, R., Eds.; The Electrochemical Society Proceeding Series; The Electrochemical Society: Pennington, NJ, 1988; p 3.
(5) Loferski, J. J.; Shewchun, J.; Mitlerman, S. D.; De Meo, E. A.; Arnott, R.; Hwang, H. L.; Beauliew, R.; Champman, G. *Solar Energy Mater.* **1979**, *1*, 213.
(6) Savell, M.; Bougnot, J. Solar Energy Conversion. In *Topics in Applied Physics*; Seraphin O., Ed.; Springer: Berlin, 1979; Vol. 31, p 213.
(7) Otamoto, K.; Kawai, S. *Jpn. J. Appl. Phys.* **1973**, *21*, 1130.
(8) Fahrenbruch, A. L.; Bube, R. H. *Fundamentals of Solar Cell, Photovoltaic Solar Energy Conversion*; Academic Press: New York, 1983; p 433.
(9) Bezig, B.; Duchemin, S.; Guastavino, F. *Solar Energy Mater.* **1979**, *2*, 53.
(10) Varkey, A. J. *Solar Energy Mater.* **1989**, *19*, 415.
(11) Sartale, S. D.; Lokhande, C. D. *Mater. Chem. Phys.* **2000**, *65*, 63.
(12) Scharifker, B.; Rugeles, R.; Mozota, J. *Electrochim. Acta* **1984**, *29*, 261.
(13) Vasquez Moll, D.; de Chialvo, M. R. G.; Salvarezza, R. C.; Arvia, A. J. *Electrochim. Acta* **1985**, *30*, 1011.
(14) Engelken, R. D.; McCloud, H. E. *J. Electrochem. Soc.* **1985**, *132*, 567.
(15) de Tacconi, N. R.; Rajeshwar, K.; Lezna, R. O. *J. Phys. Chem.* **1996**, *100*, 18234.
(16) Avey, A. A.; Hill, R. H. *J. Am. Chem. Soc.* **1996**, *118*, 237.
(17) Collisi, U.; Strehblow, H. H. *J. Electroanal. Chem.* **1990**, *284*, 385.
(18) Bard, A. J.; Faulkner, L. F. *Electrochemical Methods. Fundamentals and Applications*, 2nd ed.; John Wiley & Sons, Inc: New York, 1999; p 231.
(19) Nicholson, R. S.; Shain, I. *Anal. Chem.* **1964**, *36*, 706.
(20) Córdova, R.; Gómez, H.; Schrebler, R.; Cury, P.; Orellana, M.; Grez, P.; Leinen, D.; Ramos-Barrado, J. R.; Del Río, R. *Langmuir* **2002**, *18*, 8647.
(21) Pourbaix, M. *Atlas of Electrochemical Equilibria in Aqueous Solutions*, 2nd ed.; National Association of Corrosion Engineers: Houston, TX, 1974; p 545.
(22) Charlot, G. *L'analyse qualitative et les réactions en solutions*, 4th ed.; Masson & Cie: Paris, 1957; pp 298−311.
(23) Beaunier, L.; Cachet, H.; Froment, M.; Maurin, G. *J. Electrochem. Soc.* **2000**, *147*, 1835.
(24) Armstrong, R. D.; Harrison, J. A. *J. Electrochem. Soc.* **1969**, *116*, 328.
(25) Southampton Electrochemistry Group. *Instrumental Methods in Electrochemistry*; Ellis Horwood: Chichester, U.K., 1985; Chapter 3.